CONF-870424--14

Received by net

JUL 0 8 1987

THE INTEGRAL FAST REACTOR (IFR) CONCEPT:
PHYSICS OF OPERATION AND SAFETY

D. C. Wade and Y. I. Chang
Argonne National Laboratory
9700 S. Cass Avenue
Argonne, Illinois 60439
(312)972-4858

CONF-870424--14

DE87 011533

The submitted manuscript has been authored by a contractor of the U.S. Government under contract No. W-31-109-ENG-38. Accordingly, the U. S. Government retains a nonexclusive, royalty-free license to publish or reproduce the published form of this contribution, or allow others to do so, for U. S. Government purposes.

MASTER

DISTRIBUTION OF THIS DOCUMENT IS UNLIMITED

THE INTEGRAL FAST REACTOR (IFR) CONCEPT:
PHYSICS OF OPERATION AND SAFETY

D. C. Wade and Y. I. Chang
Argonne National Laboratory
9700 S. Cass Avenue
Argonne, Illinois 60439
(312)972-4858

ABSTRACT

The IFR concept employs a pool layout, a U/Pu/Zr metal alloy fuel and a closed fuel cycle based on pyrometallurgical reprocessing and injection casting refabrication. The reactor physics issues of designing for inherent safety and for a closed fissile self-sufficient integral fuel cycle with uranium startup and potential actinide transmutation are discussed.

I.   THE IFR CONCEPT

The key features of the IFR concept include a pool plant layout, U/Pu/Zr metallic alloy fuel, high internal conversion ratio core designs, and pyrcmetallurgical fuel reprocessing with remote injection casting fuel refabrication. The focus of IFR development is on addressing safety by providing for inherent processes to bring the core to a safe shutdown condition and to remove decay heat in response to off-normal conditions, and on addressing competitive fuel cycle economics -- even for a small scale deployment -- by employing a closed fissile self-sufficient fuel cycle based on pyrometallurgical processing and injection casting re-fabrication in a compact fuel cycle facility which can be collocated with the reactor plant if desired. The reactor physics issues of designing for inherent safety and for a closed integral fuel cycle with optional uranium startup and potential actinide self-consumption are the focus of this paper.

II. PHYSICS OF INHERENT SAFETY

The two goals of inherent safety are core reactivity shutdown and decay heat removal, both without reliance on devices requiring switching and/or outside sources of power. If moreover, it is possible to achieve both goals independent of the state of the balance of plant (BOP), then capital cost benefits can accrue by relaxing the requirement for safety grade construction of the BOP structures and components.

The requirements for removal of decay heat by inherent means include:
a) arranging the reactor vessel internals and primary coolant circuit so as to achieve natural circulation cooling of the core at the decay heat level, and a smooth transition to natural circulation upon both scrammed and unscrammed loss of primary and secondary pumping action, b) providing for an inherent decay heat removal path to an ultimate heat sink with a cooling capacity sized for the decay heat power existing after several tens of hours following shutdown, and
c) providing a thermal mass of the reactor pool and internals sufficient to absorb within structural temperature limits, that initial transient decay heat which exceeds the inherent decay heat removal capacity.

Inherent decay heat removal has been approached in the U.S. modular sized plants by use of a pool layout, suitable surface to volume ratio of the reactor vessel with natural draft air cooling of the vessel surface, elevations and redans which promote natural circulation through the core, pump coastdown time balanced to achieve smooth transition to natural circulation in both scrammed and unscrammed shutdowns, and thermal mass of the pool contents sufficient to absorb that transient decay heat which exceeds the natural draft air cooling capacity. This facet of inherent safety is discussed more fully elsewhere.[1]

Inherent control of reactivity in the face of off normal events without reliance on control rod scram has been approached in the IFR by core design for favorable ratios of the power, power to flow, and inlet temperature coefficients of reactivity and by design for a high internal conversion ratio. It will be shown below that by increasing the values of the power/flow coefficient and of inlet temperature coefficient relative to the value of the power coefficient of reactivity, it is possible to inherently bring the power to a safe shutdown level with a core average temperature rise which is well below that rise causing sodium boiling or structural damage. The use of the IFR sodium-bonded U/Pu/Zr metal alloy fuel pin has been the key means for reducing the power coefficient -- (as a result of reducing the Doppler reactivity vested in the incremental temperature rise of the fuel above the coolant). Further, the high breeding potential of the U/Pu/Zr metal alloy fuel owing to a hard neutron spectrum and a high effective density of U238 is the key feature which facilitates core designs having zero burnup control swing to minimize the potential for reactivity addition through rod runout. The rationale for this approach and the neutronics design choices taken to achieve these ends are the focus of this section.

A.   Core Physics of Inherent Shutdown

An LMR reactor core can be influenced by external events only through changes in the coolant inlet temperature and flow rate or through externally induced reactivity changes owing to control rod motion or seismically induced core geometry changes. Of these three communication paths, the BOP can influence the core only through coolant inlet temperature. These three all-encompassing paths by which external changes can influence the reactor, are embodied in the three traditional ATWS events; Loss-Of-Flow without scram (LOF), Loss-Of-Heat-Sink without scram (LOHS), and rod runout Transient OverPower (TOP) plus two overcooling accidents: pump overspeed and chilled T_{inlet}.

Given the limited ways the core can be influenced by external events, it is useful to write a quasi-static reactivity balance[2] as:

$$0 = -\Delta\rho = (P-1)A + (P/F-1)B + \delta T_{in}C - \Delta\rho_{ext} \qquad (1)$$

where P and F are normalized power and flow, δT_{in} is the change from normal coolant inlet temperature, and $\Delta\rho_{ext}$ is the externally-imposed reactivity. Here C (¢/°C) is the inlet temperature coefficient of reactivity, (A+B) (¢) is the reactivity decrement experienced in going to full power and flow from zero power isothermal at coolant inlet temperature, B (¢/100% P/F) is the power/flow coefficient, and A is the net (power-flow) (¢) reactivity decrement. In transients which are slow enough to preclude nonequilibrium stored energy in the fuel pins and delayed neutron nonequilibrium, Eq. (1) can be solved for the new power level after inherent adjustment of the reactor core to a new set of externally-controlled conditions of coolant flow, inlet temperature, and externally induced reactivity. The power adjusts up or down to compensate through the power coefficient any reactivity change caused by external events. The use of the formula can be illustrated for the case of an oxide-fueled LMR for

which the typical coefficient values are A = -$1.50, B = -$0.50, and C = -$0.005/°C. In order to reduce power from 100% to 5% by inherent means (i.e. with no rod motion) at constant flow, Eq. (1) requires that the inlet temperature must rise by 380°C as follows.

$$0 = (0.05-1)(1.50) + (0.05/1-1)(0.50) + \delta T_{in}(0.005) + 0$$

$$\delta T_{in} = \frac{1}{0.005}(1-0.05)(2.00) = 380°C.$$

In words: 95% of the $2.00 power decrement (A+B) will be introduced as a positive reactivity when the power is reduced to 5%; in the absence of control rod insertion, this positive reactivity must be compensated inherently by the negative reactivity resulting from a rise in core average temperature. The end state is a core which is critical at low power and elevated temperature. This simple example suggests that a small negative power decrement is better than a large one when inherent means (i.e. core temperature rise) are to be used to bring the reactor to a safe shutdown condition because if the temperature rise required to bring the power to zero is too large, it may induce sodium boiling, fuel element failure or structural damage to reactor components.

The above simple methodology can be used to systematically discern the desirable relationships between the reactivity parametrics, A, B, and C for the several events which encompass all possible ways the external world can affect the reactor core. Once the desired trends in A, B, and C are known, core design choices to achieve these trends can be selected. First, for the LOHS event, the scenario is that the balance of plant heat rejection is lost as a result of a feedwater pump failure or a dump of the secondary sodium to the sodium water reaction tank. This causes the inlet temperature to increase while flow remains constant; the negative reactivity induced by the inlet temperature rise is compensated by a positive reactivity due to power decrease; as power decreases, the power/flow ratio decreases and thus T_{out} collapses onto T_{in}. In the asymptote, the reactivity balance, Eq. (1), gives:

$$\delta T_{in} = \frac{(A+B)}{C} ; \quad \delta T_{out} = \delta T_{in} - \Delta T_c = \left(\frac{A+B}{C\Delta T_c} - 1\right)\Delta T_c \tag{2}$$

Here ΔT_c is the coolant temperature rise at nominal full power/flow ratio. For the LOHS, it is clear that core temperature rise will be minimized if the core is designed for a small power decrement (A+B) and a large inlet temperature coefficient (C).

Consider next the case of a Transient Overpower Event (TOP). For this scenario it is assumed that a single control rod runs out introducing a positive reactivity, $\Delta\rho_{TOP}$, while reactor coolant flow and inlet temperature remain fixed. This positive reactivity is compensated in the short term by the negative reactivity of a power increase and an increase in the power/flow ratio causing T_{out} to increase. Equation (1) gives:

$$P = 1 - \frac{\Delta\rho_{TOP}}{(A+B)} ; \quad \delta T_{out} = \Delta T_c \delta\, P/F = \frac{-\Delta\rho_{TOP}}{A+B}\Delta T_c \tag{3}$$

The inlet temperature will start to rise as the balance of plant is unable to reject the higher reactor power. Assuming no balance of plant action, the inlet temperature will increase, reducing the power ideally to the nominal heat rejection level, the power/flow ratio will return to unity, and T_{out} will

increase to compensate for the increase in the inlet temperature. Thus Eq. (1) gives

$$\delta T_{in} \ = \ \delta T_{out} \ = \ \frac{-\Delta\rho_{TOP}}{C} \ . \qquad (4)$$

In the TOP case, it is clear that a low control rod worth is desirable to limit both the initial over-power and outlet temperature overshoot, and the ultimate core temperature increase. A large power decrement (A+B) is desirable to limit the initial overpower. This is in conflict with the small power decrement (A+B) desired for inherent control of the LOHS.

Next, consider the LOF event. For this scenario, it is assumed that a loss of electrical power to the primary pump results in pump rundown and a reduction in reactor flow while coolant inlet temperature and external reactivity remain fixed; the power/flow ratio increases and the core average temperature increases inducing a negative reactivity. This negative reactivity is compensated by a positive reactivity induced by a power reduction. Asymptotically, a natural circulation flow will be established if the reactor is so designed and the power will decrease to a low value such that the positive reactivity of power reduction balances the negative reactivity of core heatup due to an increased power/flow ratio. Equation (1) gives (ideally with P=0):

$$P/F \ = \ 1 + \frac{A}{B} \ ; \quad \delta T_{out} \ = \ A/B \ \Delta T_{C}. \qquad (5)$$

For the LOF case, inherent shutdown will be promoted without large temperature rises if A, the net (power-flow) decrement is small and the power/flow coefficient (B) is large.

In the short term, the LOF transient involves dynamics effects which cause net reactivity to depart from equilibrium -- temporarily invalidating Eq. (1). Without special design measures, the pump flow coastdown time constant, τ, is shorter than the delayed neutron time constant, $1/\lambda$. Thus, when the power/flow increases and causes a negative reactivity, the compensating power reduction is not realized immediately because of delayed neutron holdback of the power decrease. The power/flow mismatch is thus exacerbated, causing an outlet temperature overshoot which relaxes out after several delayed neutron lifetimes as the reactivity because less negative, returns to zero, and establishes the asymptotic result given by Eq. (5). While the T_{out} overshoot relative to its asymptotic value cannot be quantified without dynamic analysis, it can be shown[2] that the relative overshoot is reduced when:

$$\tau\lambda(1 + A/B)^{2}|B| \ \gg \ 1\$ \qquad (6)$$

Thus, to minimize the maximum outlet overtemperature in a LOF one should reduce the asymptote by making A/B small and/or should extend the pump coastdown to reduce the overshoot relative to the asymptote or should do both.

Of the two overcooling accidents it is necessary to consider only the chilled inlet temperature case because the short term response to the pump overspeed accident does not increase outlet temperature; rather the inherent response increases power to partially return reactor outlet temperature back to

its nominal value.* For the chilled inlet temperature scenario -- which is the inverse of the LOHS -- it is assumed that a steamline rupture overcools the secondary sodium which in turn overcools the primary core inlet temperature. At constant pump flow the resulting reactivity increase is compensated by a power increase with resultant core temperature rise increase. Equation (1) gives:

$$P = 1 + \frac{C}{A+B}(-\delta T_{in}); \quad \delta T_{out} = (\frac{C\Delta T_c}{A+B} - 1)(-\delta T_{in}). \tag{7}$$

In this case core outlet temperature increase is reduced by a large power decrement (A+B) and a small inlet temperature coefficient. As expected, this is in exact opposition to the desired trends of A, B, and C in the case of the LOHS. A conservative upper bound exists on the maximum reactivity which could be introduced in such an event in that T_{inlet} cannot go below the sodium freezing temperature of the secondary sodium. If that limit were reached, the accident would revert to a LOHS accident. Thus, for typical LMR conditions of T_{in} near 350°C and ΔT_c near 150°C, the conservative upper bound is Max $\{|-\delta T_{in}|\} \leq 1.5 \Delta T_c$.

Table 1 summarizes the results for all cases and shows the desirable trends in reactivity parameters A, B, and C so as to limit the temperature increase in inherently controlled responses to all possible ways external events can influence the reactor core. Conflicts in desired trends are seen to exist for the power decrement, (A+B), concerning asymptotic and short term temperature limits in the LOF and TOP. The conflict must be resolved in favor of the long term objective while addressing the short term temperature overshoots in the TOP and LOF by design for small $\Delta\rho_{TOP}$ and suitably long pump coastdown τ. This selection is intuitively sensible when inherent shutdown is the goal because a power level reduction to the desired end state (i.e. - zero power) should introduce only a small positive reactivity -- because that reactivity must eventually be compensated by a core temperature increase.

A conflict also exists in the case of the inlet temperature coefficient. Some plausible BOP events can increase T_{inlet} and reduce reactivity (i.e. LOHS) in which case C should be large while other plausible events can decrease T_{in} and increase reactivity (i.e. steamline rupture) in which case C should be small. The inlet temperature coefficient is the only means by which the BOP can influence the core reactivity. Thus, if in addition to assuring inherent shutdown, it is also desired to achieve this irrespective of the state of the BOP, the choice of value for the inlet temperature coefficient is the place to achieve that goal. The resolution of this conflict requires a balance which is best appreciated after the discussion of the following paragraph; C should be large enough to inherently bring power to zero with acceptable outlet temperature in a LOHS but not so large that a plausible overcooling accident can lead to outlet temperature higher than those already suffered in a TOP or LOF. The choice is influenced by the value of A/B.

In Table 1 the outlet temperature increase is expressed in units of nominal coolant temperature rise ΔT_c as a function of ratios of A/B, $C\Delta T_c/B$, and

---

*Eventually, the inlet temperature and outlet temperature would rise, as in the TOP, because of the BOP's inability to reject the higher power level, and the power would return to normal with $\delta T_{out} = \delta T_{in}$.

$\Delta\rho_{TOP}/B$. Knowing that an outlet temperature margin of ~$3\frac{1}{2}$ ΔT_c exists to coolant boiling and that, for long term exposure, a margin of ~$1\frac{1}{2}$ ΔT_c exists to structural damage, it is possible to set down a set of core design goals which, while not necessary, are sufficient to promote inherent shutdown. These are

Goal	Rationale
a) A, B, and C should be negative	o negative A implies a negative prompt power coefficient o negative B and C imply a negative temperature coefficient
b) A/B should be small, eg. $\leq$ 1	o A/B must be small to inherently control the asymptotic temperature rise in a LOF
c) $C\Delta T_c/B$ should lie between one and two	o This range, with items (a) and (b), should provide a proper balance between the LOHS and chilled inlet temperature inherent responses thereby assuring inherent reactivity control for any conceivable BOP state
d) $\Delta\rho_{TOP}/|B|$ should be small eg. $\leq$ 1	o $\Delta\rho_{TOP}/|B|$ must be small to inherently control the TOP
e) $\tau\lambda(1 + A/B)^2|B|$ should be large relative to one dollar of reactivity	o Pump coastdown time, τ, should be suitably adjusted relative to delayed neutron decay time so as to minimize outlet temperature overshoot relative to the asymptote in a LOF.

B.   Core Design Choices which Promote Inherent Shutdown

        The values of the ratios, A/B, $C\Delta T_c/B$, and $\Delta\rho_{TOP}/B$ can be substantially affected by the choices made in the core design. Knowing what the trends should be to promote inherent shutdown and to suitably decouple the reactor core from the BOP, we here discuss the core design choices made in the IFR concept to achieve the desired trends.

        The definitions of the reactivity parameters, eg. $B = -\dfrac{\partial\Delta\rho}{\partial P/F}$, $C = -\dfrac{\partial\Delta\rho}{\partial T_{in}}$, etc. can be used to express A, B, and C in terms of physical reactor phenomena such as Doppler coefficient of reactivity, α_D; sodium density coefficient, α_{Na}; fuel axial expansion coeff, α_E; etc. The resulting definitions of A, B, and C in terms of physical reactivity components are displayed in Fig. 1. For example, the net (power-flow) decrement, A, is equal to the Doppler plus fuel axial expansion coefficients of reactivity multiplied by the incremental temperature rise of the fuel relative to the coolant*; the dimensions of A is

───────────────

*Whether α_e goes in A or not depends on whether the fuel is free of the clad (fuel elongation depends on fuel temperature and α_e goes in A) or is linked to the clad (fuel elongation depends on clad i.e. coolant temperature and α_e does not go in A). For metal fuel, linkage to the clad occurs after several atom percent burnup.

dollars of reactivity, and A ranges in value from 25¢ to $2.00 for current LMR designs. The power/flow coefficient, B, adds to the Doppler and fuel axial expansion coefficients additional terms due to sodium density, above core load pad thermal dilation (i.e. core radial expansion), and control rod driveline expansion all multiplied by the average coolant temperature increment relative to the inlet coolant temperature; its dimensions are dollars of reactivity per 100% in power/flow, and the range of values is 25¢ to 75¢ for current LMR designs. The inlet temperature coefficient, C, contains terms due to Doppler, fuel axial expansion, sodium density, and grid plate thermal dilation (core radial expansion); its units are $/°C and typical values are about ½ cent/°C. Figure 1 indicates the size ranges of the individual terms for typical LMR modular cores fueled with mixed oxide and fueled with U/Pu/Zr metal alloy fuels; all α's have units of $/°C and all except α_{Na} are negative.

It is evident that the three integral reactivity parameters, A, B, and C and the TOP initiator, given by:

$$\Delta\rho_{TOP} = \frac{(\text{Burnup Control Swing})}{(\text{Number of Control Rods})} * \left(\begin{array}{c}\text{1st rod out}\\\text{interaction factor}\end{array}\right) \qquad (7)$$

are all closely interrelated -- any core design choice will affect the values of them all. As a result, making design choices so as to achieve the trends which promote inherent shutdown (small A and $\Delta\rho_{TOP}$ and large B and C) requires a global core design strategy with the compromises clearly in view. The core design principles chosen for the IFR are indicated at the bottom of Fig. 1. Some terms are controlled by considerations outside the core design (eg. coolant temperature rise) and so are taken as is; some terms need to be both large and small -- the compromise is to take them as is; some compromises have a clear priority ranking (eg. the need to minimize $\Delta\rho_{TOP}$ dominates the need to make rod driveline axial expansion worth, α_R, large); but even with the necessary compromises, the introduction of the IFR metallic fuel form provides the key design variable enabling a design solution to enhance inherent shutdown performance. Specifically, A and $\Delta\rho_{TOP}$ can be made small by choice of the metallic fuel form and B and C can be made large by core layouts which enhance axial and radial leakage. These selections are elaborated on below.

The net (power-flow) decrement (A) is given by

$$A = - (\alpha_D + \alpha_E)\overline{\Delta T}_f \qquad (8)$$

As shown in Fig. 1 the fuel Doppler and fuel axial expansion coefficients affect the values of B and C (which should be made large) as well as A (which should be made small). However, the incremental temperature rise in the fuel $\overline{\Delta T}_f$, which acts on these reactivity coefficients, appears in A only and is used as the key design variable to achieve a low value of A. Because of the factor of ten higher thermal conductivity of metal fuel relative to mixed oxide and because of the sodium bond, metallic fuel pins enjoy a very low $\overline{\Delta T}_f$ at characteristic LMR conditions (eg. 0.30 inch pins and 15 kW/ft peak linear heat rating $\overline{\Delta T}_f \sim 150°C$). For comparable LMR designs, the net (power-flow) coefficient (A) can be reduced by factors of 6 or so (from $1.50 to 25¢) by employing the IFR metallic fuel vs. mixed oxide. Alternately, oxide pins could be derated (to 3-7 kW/ft) so as to reduce $\overline{\Delta T}_f$. The metallic fuel form has an additional favorable feature in that after 1 or 2% burnup the metallic fuel becomes bounded to the clad so that the fuel axial expansion is controlled by clad (i.e. coolant) temperature, not fuel temperature thus further reducing A by nearly a factor of two.

The power/flow coefficient, B, and the inlet coefficient, C, rely on the same physical feedback mechanisms (see Fig. 1). The design strategy taken in the IFR to make them large is to design for large net negative core radial expansion plus sodium density coefficients and take the other terms as is. Both the sodium density and the radial expansion coefficients can be made more negative by designing the core to enhance axial leakage; the positive sodium density coefficient is reduced by increasing the negative leakage component through the use of appropriate H/D ratio and also by use of heterogeneous layouts. The negative radial expansion coefficient (due to increasing core interassembly gap upon core support thermal dilation) becomes more negative as the axial leakage fraction is increased and is thus also sensitive to H/D. Thus, the IFR design strategy is to hold height to diameter, H/D, ratios on core dimensions in a range favoring axial leakage and to employ heterogeneous core layouts to further reduce the sodium density coefficient. The heterogeneous layouts increase the enrichment, thus reducing the Doppler coefficient and thereby further contribute to a reduction in A/B.

The desired trend, $1 \leq C\Delta T_c/B \leq 2$, needed to provide inherent safety in both LOHS and chilled inlet temperature accidents and to suitably decouple reactivity from BOP events is achieved automatically since

$$\frac{C\Delta T_c}{B} = \frac{2}{1 + \frac{\left(\frac{4}{3}\alpha_B - \alpha_g + 2\alpha_R\right)}{C}} = \frac{2}{1 + (0 \leq \# \leq 1)}$$

The extra terms in the dominator are small relative to C because the control rod driveline expansion reactivity is small in cores designed for small $\Delta\rho_{TOP}/B$ and the above core load pad and grid plate radial expansion coefficient terms nearly cancel.

The TOP initiator could be made small either by increasing the number of control rods or by designing for reduced burnup control swing. The design strategy taken for the IFR is to design for high internal conversion by maximizing the U238 content of the core and maximizing the effective η of the fuel (neutrons released per neutron absorbed in the fuel) by hardening the spectrum. High internal conversion designs are favored by various combinations of large pins, internal blankets, hard spectrum, and low enrichment. Again the IFR metallic fuel form provides unique advantages in both high effective U238 number density and in large effective η. For example, in an internal blanket assembly with 50% fuel volume fraction, U/Zr metallic alloy pins at 85% smear density provide 35% more U238 atoms than will UO_2 pins at 93% smear density and 97.7% pellet density. Additionally, as shown in Table 2, the harder spectrum achievable in a metal fueled core provides 20% more excess neutrons available for breeding (because of smaller fissile α and more fertile fast fissions) than are available in the softer mixed oxide spectrum.

C.   Summary: IFR Design Strategy for Inherent Shutdown

The IFR neutronics core design strategy for achieving inherent shutdown rests on the principals developed above. The resulting designs have as their key feature the use of the U/Pu/Zr metallic fuel form. The high thermal conductivity of this fuel minimizes the reactivity vested through Doppler in the net (power-flow) decrement A relative to that vested in the power to flow reactivity coefficient, B. Further, the high effective heavy metal density and the hard neutron spectrum achievable in cores using the U/Pu/Zr fuel form make possible high internal conversion ratio designs which have nominal zero burnup control

swing and essentially zero TOP initiator even with 4 to 5 years fuel residence time and 12 to 20 month refueling interval.

The IFR approach has been applied to cores ranging in size from 400 MWth through 3700 MWth. For consistency, numerical examples of IFR performance quoted here and in the following sections are based on a 900 MWth modular reactor design, shown in Fig. 2, the salient properties of which are listed in Table 3. This core is described more fully in Refs. 3 and 4. A version of this core modified to achieve higher internal conversion ratio is shown in Fig. 3. This modification has a two inch taller core, 9 more internal blankets, 6 less drivers, 3 less secondary control rods and 85% vs. 75% smear density in the blanket pins.

The inherent safety parameters achieved in the reference (Fig. 2) design are shown in the first column of Table 4. It is seen that the sufficient-condition goals for inherent shutdown were met by the neutronics design choices. Detailed plant wide model dynamic simulations of the response of this core to the several ATWS events have confirmed[5] the adequacy of the inherent feedbacks in controlling reactivity and maintaining core outlet temperatures in the acceptable range.

II. PHYSICS OF THE INTEGRAL FUEL CYCLE

A. IFR Fuel Cycle Based on Pyrometallurgical Reprocessing

The metallic fuel form facilitates the use of a pyrometallurgical process for fuel reprocessing[6] wherein the fuel remains in a metallic form throughout the process, the uranium and plutonium remain intimately mixed, and the fission product removal fractions are 10 to 100 times less than in aqueous processes. Figure 4 summarizes the process; blanket elements and driver elements go through separate electrorefining operations wherein the cladding and fission products are separated into the salt phase and the uranium and plutonium are deposited in metallic form on cathodes. The cathode from the blanket process is subjected to a halide slagging step to separate a plutonium-rich feed for fissile makeup in driver refabrication from a uranium-rich feed for the blanket refabrication. These metallic feed streams supply a fuel and blanket remote refabrication process housed in the same hot cell and based on injection casting of fuel slugs, followed by insertion and seal welding into sodium-bonded clad.[7] The fuel cycle is operated in a closed, fissile self sufficient mode wherein the reactor breeding just compensates reprocessing/refabrication losses. The external feeds to the integral fuel cycle are depleted uranium and fuel assembly steel hardware.

Although the partition fractions and recovery factors achieved in the pyroprocesses will not be known with high precision until completion of further experiments, the main features which affect core neutronics are (1) all of the Np and Cm produced in the core and blanket assemblies go with Pu rather than the U and thus they re-appear in subsequent driver assemblies, (2) Am is removed with the fission products, (3) about 1% of the fission products are not removed, and (4) about 5% of the Pu in the burned blankets goes with the U in the halide slagging process and re-appears in subsequent blanket assemblies. Although all of the Am is expected to be removed during the reprocessing step, ^{241}Am is present when the refabricated fuel is charged to the reactor as a result of the beta decay of ^{241}Pu to ^{241}Am during the time span between the reprocessing step and element loading at the beginning of the next cycle.

Current U.S. modular core designs based on the IFR approach employ 4 or 5 year fuel residence time with 12 or 20 month refueling intervals under the expectation that the IFR fuel testing program will support average fuel burnups of 110 (150 pk) MWd/kg and $3.5 \cdot 10^{23}$ peak fast fluence. The integral fuel cycle employs a 1 year cooling period and a 6 month reprocessing/6 month refabrication cycle with subsequent reload of the assemblies.

B. Mass Flows and Neutronics of the IFR Equilibrium Fuel Cycle

An equilibrium state will eventually prevail in the IFR as a result of the closed fuel cycle with depleted uranium feed and bred fissile recycle through a core whose breeding ratio has been adjusted to just compensate the reprocessing/refabrication losses. Although this is an idealized case, the equilibrium cycle provides a well-defined, unique, and relevant basis for assessing the impacts of the partition fractions and recovery factors of the pyroprocessing chemistry upon core neutronics.

Equilibrium cycle sensitivity studies have been performed[3,4] for the 900 MWth IFR core described in Table 3 and Fig. 2. The modeling of the closed cycle employed ENDF/B-V.2 basic nuclear data and the REBUS-3 code system[8] which solves the coupled set of space dependent neutron flux and isotope depletion equations which define the mass flows of the reactor and couples those to a modeling of the cooling, reprocessing, and refabrication out-of-core components of the integral fuel cycle. The mass flows which comprise the equilibrium cycle are determined by a nested iterative process which is repeated until the isotopic splits of the feed streams out of reprocessing from the previous iteration are equal to the current iterate feed streams into refabrication, and the reactor having this composition specification meets the reactivity criteria of $k_{eff} = 1$ at EOEC and 292 days (1 year, 80% capacity factor) of full power operation with 4 year residence time and annual $\frac{1}{4}$ core refueling. This equilibrium state depends on the fuel reprocessing partition and recovery fractions, the fabrication specification and losses, the reactor residence time, refueling interval, cooling interval, reprocessing time interval and refabrication time interval, as well as power level, capacity factor and isotopic split of external feedstock (i.e. depleted uranium in this case).

The burnup chain used in the model is shown in Fig. 5. The chain is terminated when a capture event occurs in ^{246}Cm so that the production and recycle of Bk, Cf and Es has been neglected. This approximation introduces little error because the bulk of these three actinides are removed along with the fission products during the electrorefining step so that buildup during the core residence time is all that is neglected.

The real, nearly-continuous (i.e. several assemblies per day) batch process size was approximated as follows: the 292 day reprocessing/fabrication time interval was split into two equal periods; 146 days for reprocessing (with the chemical separations occurring on the 146th day) and 146 days for refabrication. This affects the buildup of Am^{241} in particular and results in an approximate "time averaged" heavy metal isotopic mix for all such daughter isotopes used in the fuel loading of the subsequent burn cycle.

The REBUS code was run in the equilibrium recycle mode with the assumptions listed above so as to determine the equilibrium composition and performance of the IFR core described in Table 3. Table 5 shows the 1/6th core mass flow characteristics of the assumed fuel cycle. The composition of the charged (upper left column) and recharged (lower right column) fuel is, indeed, in equilibrium for the assumptions of the model. The table shows the surplus of

Pu^{239} and higher actinides created each cycle (column labeled "reprocessed and sold") -- which is the excess assumed adequate to handle reprocessing/refabrication losses. The inexorable buildup of the products of higher actinide parasitic capture (Bk, Cf and Es) are eliminated with the fission product waste stream.

In order to show the sensitivity of reactor performance and of mass flows to the partition and recovery fractions assumed for the pyroprocess, the calculations were rerun using an altered set of fuel cycle assumptions. Here the Am as well as the Np and Cm produced in the core and blanket were assumed to be recycled (rather than Np and Cm only), all fission products were assumed removed, and the Pu carry over with U during halide slagging was assumed to be zero. The modified assumptions yield a much higher Am and Cm core inventory -- 29.45 kg vs. 1.60 kg -- up to 0.4% of the total core heavy metal inventory. The increase in the higher actinide inventory results from the assumed non removal of Am during reprocessing because the isotope, ^{241}Am, on the principal chain leading to Cm has been recycled and is available for transmutation (i.e., ^{241}Am capture to ^{242}Am, β' to ^{242}Cm; see Fig. 5). In general, the results show that the actinide concentrations are a factor of 3 to 10 higher when compared to the reference solution.

Table 6 compares some of the reactor performance parameters for the two cases. As expected the reference (former case) displays slightly degraded performance relative to the modified case where fission products are assumed to be totally removed and higher actinide buildup (i.e. Am recycle) is enhanced; in particular, the breeding ratio is slightly lower and the reactivity burnup swing is larger by 0.04% Δk. This is due not only to the fission product poisoning but also to the fact that the microscopic nu-fission cross sections of the higher actinides which build up if Am is recycled are larger than the nu-fission cross section of the Pu's. Recycling of 5% of the discharged blanket Pu back into the blanket in the reference case had little effect on the power production characteristics of the blanket.

In general, it is found that the IFR reactor neutronics performance parameters in the integral fuel cycle are not highly sensitive to variations in the partition and recovery fractions of the pyroprocess and injection casting refabrication steps so that future detailed core designs can easily accommodate to changes as these parameters become better known through the IFR pyroprocess development program.

C. Physics Impacts of Optional Actinide Self Consumption and Non TRU Waste Streams

An optional actinide stripping post process on both the metal and salt waste streams from reprocessing has been proposed[9] so as to yield only non TRU external waste streams from the IFR fuel cycle. The residual Pu and higher actinides stripped from the waste would be mixed into the refabrication feed streams for recycle into the core for transmutation. The stripping process, however, is expected to carry over an as-yet undetermined fraction of the lanthanide fission products along with the actinides. These would then be recycled into the core also.

The core physics aspects of operating the reactor in such an actinide self consumption mode with partial lanthanide recycle has been evaluated using the modeling of the fuel cycle described above. In this case total actinide recycle was modeled, with lanthanide recycle treated parametrically. The total lumped fission product recycle fraction, F_E, in the REBUS equilibrium cycle

· modeling is given as $F_E = RA/(A + (1-A)(1-R))$ where A is the fraction of fission product absorptions attributable to lanthanides (~1/3) and R is the fraction of lanthanides which carry over in the actinide stripping step on the waste stream. The results of the parametric study are summarized in Table 7 which shows the resulting impact on core performance. It is clear from these results that total actinide self consumption with unavoidable lanthanide recycle of up to even 40% could be easily accommodated from the core neutronics point of view. Recycle in either driver or blanket assemblies would be optional.*

D.   Option for High Breeding

Current applications of the IFR concept to U.S. modular core designs employ a fissile self sufficient closed integral cycle with just enough breeding to overcome reprocessing and refabrication losses. High internal conversion ratio is stressed to achieve inherent safety in TOP events while breeding in external blankets is minimized. A radially heterogeneous layout has been used to promote the high internal conversion ratio as well as to achieve a high power/flow reactivity coefficient through minimizing sodium density coefficient. Only a single row of radial blankets is used, and the driver assemblies have no axial blankets.

However, dramatic flexibility exits in the use of the IFR metallic fuel to accommodate to changing economic and/or energy demand needs. By the simple addition of axial blankets and the exchange of radial shield for radial blanket assemblies, breeding ratios of >1.5 are achievable -- with no change in core layout or assembly design and with only small change in core performance. Table 8 compares key physics performance parameters for the core designed for fissile self-sufficiency and defined in Table 3 and Fig. 3 with a core modified only by the addition of 14 inch axial blankets, exchange of 2 rows of radial shield with blanket to given 3 rows of blanket, and extension of radial blanket residence time from 4 years to 6, 9, and 12 years for the first, second, and third rows, respectively. The changes in core performance attendant the dramatic increase in breeding ratio from 1.13 to 1.55 are small and are generally favorable owing to a reduction in core power fraction. The increased burnup control swing and attendant increase in TOP initiator while, too large for excellent inherent performance in the case shown here, would be reduced by a small decrease in the radial and internal blanket smear fraction in a refined design.

E.   Option for Startup on U235 Fuel

While plutonium fueling of the startup core would be employed if economics and fuel supply favored it, the option to fuel the initial core and first reload with U^{235} and to subsequently maintain fissile self sufficiency in the closed integral fuel cycle transition to an equilibrium plutonium cycle provides for both an assured fuel supply in the current U.S. no-reprocessing environment and for a known and stable upper bound on the projected cost of the initial fissile loading. The pyroprocessing and injection casting refabrication processes are applicable equally and with virtually no change to either U235 or Pu fissile material in the U/Zr or U/Pu/Zr metal alloy fuel, and the IFR fuel pin irradiation development program is addressed at both materials.

---

*The metallurgical impact of such actinide and lanthanide recycle on fuel pin morphology and pin/clad chemical compatibility has not as yet been evaluated.

From the core design and core neutronics point of view, the goals for the uranium startup option are to maintain the core layout and the assembly and pin designs unchanged throughout the period of transition from uranium startup to equilibrium plutonium cycle, and to maintain fissile self sufficiency after the first several cycles. The core neutronics issues involve adequacy of core static performance (power peaking, burnup swing, adequacy of control rod worth) and inherent safety performance (impact of changing β, reactivity feedback coefficients, and burnup control swing -- i.e. TOP initiator) throughout the whole of the transition to the equilibrium Pu cycle.

The reference core design of Table 3 and Fig. 2, which was optimized for the closed equilibrium Pu cycle, was used to investigate the uranium startup option. A scatter reload (no fuel or blanket shuffling) fuel management pattern was developed for the equilibrium Pu cycle wherein about ¼ of the core and blanket was refueled each year (see the refueling sequence in Fig. 2.). This core, with a breeding ratio of 1.04 was just fissile self sufficient for the assumed reprocessing/refabrication losses. An initial loading of this exact same core was then fueled with U/Zr metallic fuel in the pins rather than U/Pu/Zr fuel, and the same fuel reload pattern was executed for 18 cycles. The first two cycles were fueled with U235. In subsequent cycles the isotopic mix and available fissile mass of the fuel feed for each cycle's loading was based on the Pu isotopics of the twice previous cycle's discharge (and if a fissile deficit existed it was made up with U235). Figure 6 illustrates the resulting variation of the isotopic makeup of the core fissile loading; the gradual replacement of the U235 in the core loading by recycle Pu is evident -- with the fissile-Pu concentration equaling that of U235 by cycle 10 and exceeding it by approximately a factor of three by cycle 18. The core fissile mass and reload enrichment decreases as the Pu concentration in the charged fuel increases relative to the less reactive U235.

The breeding ratio for the initial core was 0.685, increasing to 0.792 by cycle 9 and to 0.906 by cycle 18. Although a breeding ratio less than 1.0 during transition does not preclude a regenerative fissile fuel cycle -- because the reactivity worth of the bred Pu exceeds that of U235, -- the self-sufficiency during the transition was, in fact, slightly deficient in the core designed for a breeding ratio of 1.02 in the equilibrium Pu cycle. The fissile deficit at the end of 18 cycles, accounting for the relative worths of fissile isotopes, was found to be approximately 190 kg. This deficit accumulated mostly early in the transition and at an ever decreasing rate as the reactor breeding ratio approached the equilibrium-cycle value.

Figure 6 shows that the concentration of U236 in the core loading builds up to a significant level, comprising roughly 3.5% of the heavy metal by cycle 18. To investigate the effect of U236 on core performance, equilibrium-cycle calculations were performed using three different fissile-fuel compositions: composition A, which is the transition composition typical of cycle 15 through 18 and thus containing substantial U236; composition B, which is the same as composition A but with the U236 artificially removed; and composition C, which is the equilibrium Pu composition. Results are summarized in Table 9. The burnup reactivity swing with the equilibrium fuel is about 1.16% Δk, compared to about 1.65% Δk for the transition core containing U236 and about 1.40% Δk for the transition composition without U236. Apparently, half the difference in burnup reactivity swing between the equilibrium core and the transition core (representative of cycles 15 through 18) is caused by the presence of U236, while the other half can be attributed to the U235 content in the transition fuel. The table also shows that the decrement in breeding ratio between the equilibrium core and the late transition cores is partly due to the U236 -- which displaces

U238. Because of the significant adverse effects of U236 on core performance late in the transition, it may be desirable to eliminate uranium from the discharged core fuel once the U236 to U235 concentration ratio exceeds some specified amount.

During the first three cycles, the driver power fraction (at beginning-of-cycle) decreased from 92% to 86%, while the blanket power fraction increased as fissile Pu was bred. After the first three cycles, the driver, internal blanket, and radial blanket gradually approached their beginning-of-equilibrium Pu cycle power fractions of 82%, 12%, and 5%, respectively. The maximum driver power peaking factor during the transition was 1.67 and occurred at the beginning of cycle 7, while the largest peak linear power was 15.3 kW/ft at the beginning of cycle 3. These values are not significantly different compared from the equilibrium Pu cycle values of 1.61 and 14.3 kW/ft, respectively.

The results of this study indicate that from the point of view of core static performance, the uranium startup option is perfectly feasible. Slight core design changes from the core analyzed here to provide for slightly more breeding by an internal blanket pin smear fraction change and to provide slightly more control worth to compensate the larger burnup swing are required but pose no feasibility issue.

The impact of the uranium startup option on inherent safety performance was evaluated using the quasi static reactivity balance approach. First, since the asymptotic outlet temperature changes in response to ATWS events all are expressible as ratios of A, B, C, and $\Delta\rho_{TOP}$ -- whose units are ¢ or ¢/°C -- it is clear that the reactivity scale factor, β, divides out, and the larger delayed neutron fraction of U235 relative to Pu239 plays no role. The larger delayed fraction does affect the initial temperature overshoot in the LOF event, however. The fraction of the power attributable to delayed neutrons in the uranium core exceeds by a factor of two that for the plutonium-fueled core. This increases the delayed neutron holdback of the power reduction experienced upon negative reactivity insertion, so that in an unprotected LOF the initial power/flow mismatch is exacerbated relative to the plutonium fueled case. Numerical studies show that the outlet temperature overshoot is increased about 50°C relative to that for a Pu fueled core, and thus can be accommodated.

The reactivity coefficients themselves change when the fissile material is changed from Pu to U235 with fixed core geometry both because the enrichment goes up and because of intrinsic differences in the energy dependence of the cross sections of the two fissile materials. Table 10 summarizes the results and shows that in going to the uranium fueled core, the sodium density coefficient becomes negative and the Doppler, radial, and axial expansion coefficients become about 10% less negative. When combined into the relevant inherent safety parameters A, B, and C and used in the quasi static formulas it is shown in the second column of Table 4 that the uranium startup core would experience no substantive difference in the asymptotic outlet temperatures attained in unprotected LOF and LOHS accidents.

The burnup control swing in the uranium fueled core is about 60% greater than in the plutonium fueled core when expressed in %Δk units. However, because of the roughly 100% increase in β, the burnup swing expressed in ¢ is smaller and the TOP would be milder. However, a difference in metallurgical properties of the U/Zr and U/Pu/Zr fuel alloys counteracts this trend. Both alloys experience axial fuel growth in response to fission gas induced swelling; the resulting fuel column growth peaks at about 1 to 2 atom percent burnup with the binary alloy elongating 8% whereas the plutonium bearing alloy elongates only

3%. The increased elongation of the uranium startup fuel adds roughly 0.5% Δk to the burnup control swing* requiring higher enrichment and deeper initial insertion of the control rods. For the unprotected TOP ATWS event, the net effect of the larger β, larger burnup swing, and reduced power decrement (A+B) would lead, as indicated in Table 4, to a worst TOP power overshoot than experienced in the Pu fueled equilibrium cycle core. While the overshoot ratio required to fail fuel pins[10] or to boil coolant would not be reached, a TOP overshoot this large is undesirable from the investment protection point of view, and will require further efforts to achieve its reduction.

III. SUMMARY

The IFR concept goals include use of passive means for reactivity shutdown and decay heat removal and use of a closed integral fuel cycle based on pyrometallurgical processing to achieve low fuel cycle costs. The reactor physics issues of designing for inherent shutdown and for a closed, fissile self-sufficient fuel cycle have been examined. It is shown that inherent shutdown can be achieved by core design choices which reduce the power coefficient of reactivity relative to the power to flow and inlet temperature coefficients and which produce a high internal conversion ratio.

The use of a U/Pu/Zr metallic fuel form has been the key means for achieving these design goals. Its high thermal conductivity reduces the component of the power coefficient vested in the incremental temperature rise of the fuel pin relative to the coolant and its high effective heavy metal density and hard neutron spectrum due to no low A neutron moderator atoms permits high internal core conversion ratios.

The IFR core static neutronics performance parameters have been shown to be suitably insensitive to variations in pyroprocessing partition and recovery factors which have yet to be established with high precision. The option to start up on U235 and to transition in a fissile self-sufficient closed cycle to the equilibrium Pu cycle has been established with account taken of both core static neutronics performance and inherent safety performance throughout the transition. A fixed core layout and assembly design has been shown to be usable without change for the equilibrium Pu cycle (with or without actinide recycle for self-consumption), for optional U startup and transition cores, and for optional high breeding ratio cores where axial and radial blankets are added to the otherwise unchanged core.

---

*Computed for cycles 3 and beyond where, because of the 4 year fuel residence time with annual refueling only ¼ of the uranium driver assemblies experience the fuel growth during a 1 year reload cycle.

References

1. C. Peroulias, R. C. Gerber, and J. C. Mills, "Inherent Decay Heat Removal Performance in SAFR," Proceedings of the Conference on Science and Technology of Fast Reactor Safety, Guernsey, England, May 1986.

2. R. H. Sevy, Personal Communication, Argonne National Laboratory (October 1985).

3. Y. Orechwa, H. S. Khalil, T. B. Turski, and E. K. Fujita, "Core Design of Small Inherently Safe LMRs," Proceedings of the Topical Meeting on Advances in Fuel Management, March 2-5, 1986, Pinehurst, NC, American Nuclear Society, p. 152.

4. H. S. Khalil, E. K. Fujita, S. T. Yang, and Y. Orechwa, "Fuel Management Studies of Small Metal and Oxide LMRs," Proceedings of the Topical Meeting on Advances in Fuel Management, March 2-5, 1986, Pinehurst, NC, American Nuclear Society, p. 159.

5. J. E. Cahalan, "Safety Aspects of LMR Core Design," Proceedings of the Topical Meeting on Reactor Physics and Safety, Saratoga Springs, September 1986, p. 121, NUREG/CP-0080.

6. L. Burris, M. J. Steindler, and W. E. Miller, "A Proposed Pyrometallurgical Process for Rapid Recycle of Discharged Fuel Materials from the Integral Fast Reactor," Proceedings of the Fuel Reprocessing and Waste Management Meeting, Jackson, Wyoming, August 1984.

7. L. Burris and L. C. Walters, "The Proposed Fuel Cycle for the Integral Fast Reactor," Trans. Am. Nucl. Soc., 49, 90 (1985).

8. B. J. Toppel, "A User's Guide to the REBUS-3 Fuel Cycle Analysis Capability," ANL-83-2, Argonne National Laboratory (1983).

9. T. R. Johnson, "Personal Communication, Argonne National Laboratory, August 1986.

10. T. E. Wright, T. H. Bauer, R. K. Lo, and R. G. Palm, "Recent Metal Fuel Safety Tests in TREAT, Proceedings of the Conference on Science and Technology of Fast Reactor Safety, Guernsey, England, May 1986.

11. R. G. Pahl, C. E. Lahm, R. Villarreal, W. N. Beck, and G. L. Hofman, "Recent Irradiation Tests of Uranium-Plutonium-Zirconium Metal Fuel Elements," Proceedings of the International Conference on Reliable Fuels for Liquid Metal Reactors, Tuscon, Arizona, September 1986, p. 3-36.

Designing to Desirable Trends in Feedback Coefficients

Desire	Doppler	Fuel Axial Expansion	N_a Density	Rod Driveline	Radial Expansion	Coolant ΔT	Fuel ΔT
Small A =	$\{\ \alpha_D$	$+\ \alpha_E$					$\}*\Delta T_F$
Large B =	$\{\ a_D$	$+\ \alpha_E$	$+\ \alpha\ N_a$	$+\ 2(\alpha_R$	$+2/3\alpha_B)\}$	$*\ \Delta T_C/2$	
Large C =	$\{\ \alpha_D$	$+\ \alpha_E$	$+\ \alpha\ N_a$		$+\ \alpha_G\ \}$		
Metal	−0.10	−0.12	+0.18		−0.16 −0.33	150	150
Oxide	−0.16	−0.10	+0.11		−0.12 −0.27	150	750
Design Strategy	Take As Is	Take As Is	Make Less +	Take As Is	Make Large	Take As Is	Make Small

Fig. 1.   IFR Core Design Strategy for Inherent Shutdown
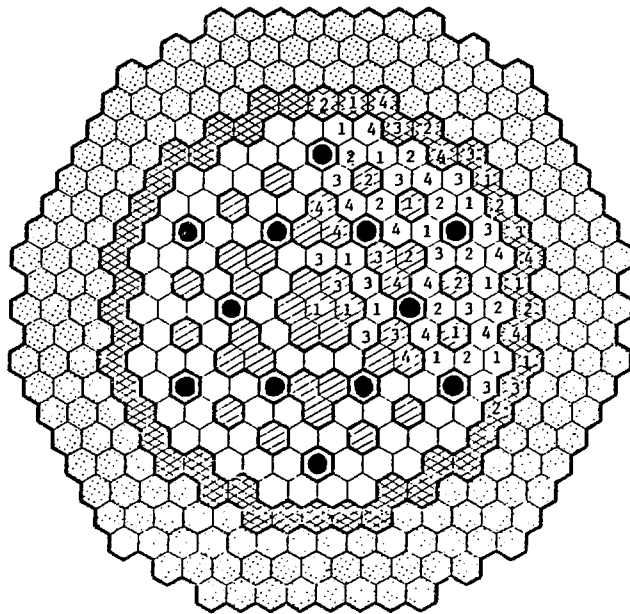
Fig. 2. 900 MWth Core Layout and Refueling Scheme
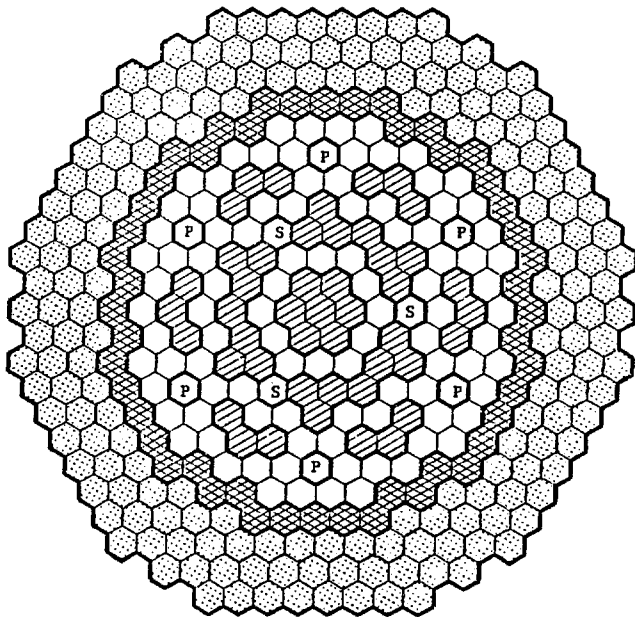
Fig. 3. 900 MWth Modified Core Layout for
High Internal Conversion Ratio

Fig. 4.   IFR Pyrometallurgical Processes for Core and Blanket

Fig. 5.   IFR Depletion Analysis Model
          (Note; the radioactive decay of ^{239}Pu and
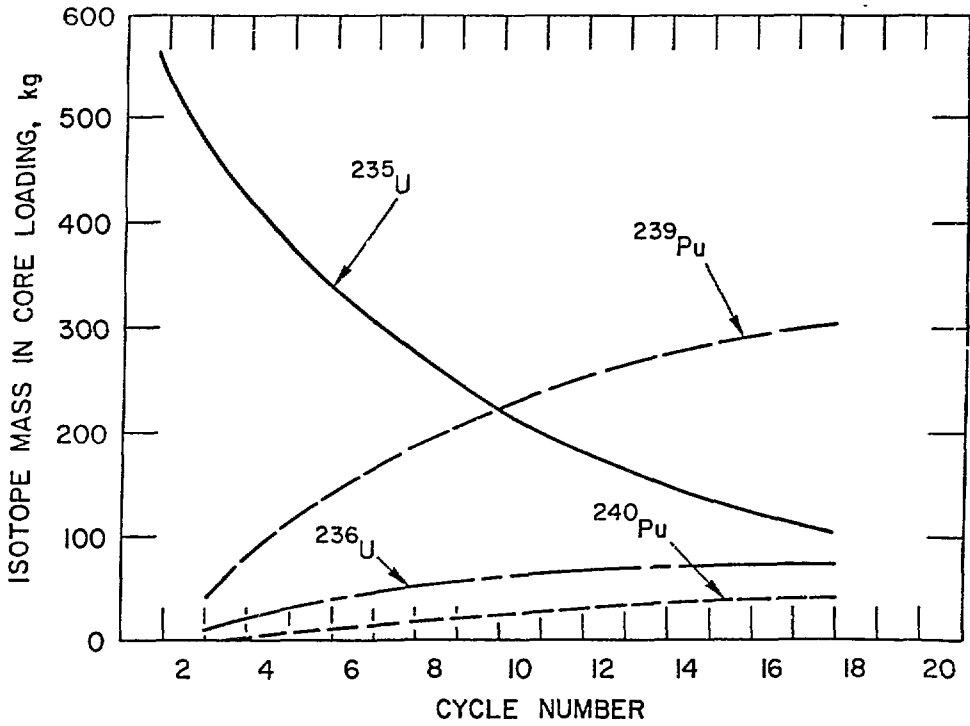 ^{239}Np is assumed to occur with no time delay)

Fig. 6. IFR Uranium Startup Transition to Equilibrium Cycle

TABLE 1. Quasi Static Reactivity Balance Results for Unprotected Accidents

	Asymptotic State				Intermediate State	Indicated Trend for Inherent Shutdown*
	P	F	δT_{in}	δT_{out}		
LOHS	~0	1	$\dfrac{A+B}{C}$	$\left(\dfrac{1+A/B}{\dfrac{C\Delta T_c}{B}} - 1\right)\Delta T_c$	Monotonic transition to asymptotic	• A+B small • C large
TOP	~1 (after rise in T_{in} due to BOP heat removal limit)	1	$\dfrac{\Delta\rho_{TOP}}{-C}$	$\delta T_{out} \approx \delta T_{in}$ $=\left(\dfrac{\Delta\rho_{TOP}/B}{-C\Delta T_{c}/B}\right)\Delta T_c$	Initial rise at constant T_{in} $P = 1 + \dfrac{-\Delta\rho_{TOP}/B}{1+A/B}$ $\delta T_{out} = \left(\dfrac{-\Delta\rho_{TOP}/B}{1+A/B}\right)\Delta T_c$	• A+B large • C large • $\Delta\rho_{TOP}$ small
LOF	~0	Natural Circulation	0	$(A/B)\Delta T_c$	overshoot relative to delayed neutron hold-back of power decay minimized if $\lambda\tau(1+A/B)^2\|B\|\gg1$	• A small • B large • τ long
Chilled Inlet	$1 - \dfrac{C\delta T_{in}}{A+B}$	1	$\|{-\delta T_{in}}\|\le(T_{inlet}$ $-T_{Na\ freeze})$ $\approx1.5\ \Delta T_c$	$\left(\dfrac{C\Delta T_{c}/B}{1+A/B} - 1\right)(-\delta T_{in})$	monotonic transition	• C small • A+B large
Pump Overspeed	$\dfrac{1+A/B}{1/F + A/B}$ (always > 1)	F>1	0	$\left(\dfrac{1}{1 + \dfrac{A/B}{1+A/B}(F-1)}\right)\Delta T_c$ (always < 0)	monotonic transition	• A negative • B negative

*Conflicts are seen to exist between desirable trends for different ATWS events.
 Resolution of these conflicts is discussed in the text.

TABLE 2. Effect of Hardened Neutron Spectrum on
Neutrons Available for Internal Breeding

	Oxide	Metal
η of Fissil Isotopes	2.283	2.450
Fertile Fission Bonus, ϵ	0.356	0.509
Total Excess Neutrons		
$\eta - 1 + \epsilon$	1.639	1.959
Total Loss	0.308	0.332
Net Neutrons for Breeding	1.331	1.627

TABLE 3. 900 MWth IFR Core Design Parameters

Reactor Power, MWth	900
Reactor Outlet Temperature, °F	950
Reactor ΔT, °F	275
Core Concept	Heterogeneous
Fuel Residence Time, Cycles	
Driver	4
Blanket[a]	4
Cycle Length, full-power days	292
Fuel Material	
Driver	U-Pu-10% Zr
Blanket	U-10% Zr
Clad and Duct Material	HT-9
Fuel Smear Density, %T.D.	
Driver	75
Blanket	75
Active Fuel Height, in.	
Driver	36
Blanket	44
Axial Blanket Thickness, in.	0.0
Number of Pins per Assembly	
Driver	271
Blanket	169
Fuel Pin Diameter, in.	
Driver	0.285
Blanket	0.392
Pin Pitch/Diameter Ratio	
Driver	1.18
Blanket	1.09
Cladding Thickness, in.	0.022
Duct Wall Thickness, in.	0.14
Interassembly Sodium Gap, in.	0.15
Assembly Lattice Pitch	6.06

[a]Refers to internal and radial blanket.

TABLE 4. 900 MW$_{th}$ Inherent Shutdown Reactivity Ratios

Parameter			EOEC Pu Fueled	BOL U Fueled
A	(¢)		-26.1	-12.3
B	(¢)		-37.2	-24.1
C	(¢/°C)		-0.376	-0.245
A+B	(¢)		-63	-36
$\Delta\rho_{TOP}$ (Fig. 3 Layout)		(¢)	6	30
A/B			0.70	0.51
$\dfrac{C\Delta T_c}{B}$			1.52	1.52
$\Delta\rho_{TOP}/\|B\|$			0.16	1.49
$\tau\lambda(1+A/B)^2\|B\|$ ($)			0.54	0.27

TABLE 5. IFR Closed Fuel Cycle Mass Flows for 900 MWth Reactor
(Flows for 1/6 core model)

EXTERNAL CYCLE SUMMARY IN KILOGRAMS

ISOTOPE	CHARGED	DISCHARGED	AFTER COOLING	SOLD	DELIVERED TO REPROCESSING	LOST IN REPROCESSING
U-234	9.37402D-04	7.11118D-03	9.04711D-03	0.0	9.04711D-03	9.03064D-03
U-235	1.34330D+00	7.39874D-01	7.39894D-01	0.0	7.39894D-01	7.15379D-01
U-236	3.78017D-03	1.21374D-01	1.21374D-01	0.0	1.21374D-01	1.17594D-01
U-238	6.87094D+02	6.37612D+02	6.37612D+02	0.0	6.37612D+02	6.17264D+02
PU238	2.96707D-01	3.07107D-01	3.14781D-01	0.0	3.14781D-01	-8.14397D-04
NP237	3.65463D-01	3.83512D-01	3.88512D-01	0.0	3.83512D-01	2.77556D-17
PU236	2.29533D-06	3.60234D-06	2.95542D-06	0.0	2.95542D-06	2.74893D-07
PU239	5.47017D+01	5.81301D+01	5.81301D+01	0.0	5.81301D+01	-5.03980D-06
PU240	1.74135D+01	1.85186D+01	1.85193D+01	0.0	1.85193D+01	-3.45966D-04
PU241	2.00143D+00	2.29553D+00	2.21040D+00	0.0	2.21040D+00	4.12993D-02
PU242	9.14443D-01	9.72712D-01	9.72712D-01	0.0	9.72712D-01	0.0
AM241	3.81073D-02	2.67479D-01	3.52453D-01	0.0	3.52453D-01	3.52453D-01
AM242	0.0	9.84051D-03	9.84051D-03	0.0	9.84051D-03	9.84051D-03
AM243	0.0	8.29122D-02	8.29122D-02	0.0	8.29122D-02	8.29122D-02
CM242	1.07790D-03	1.37797D-02	3.97479D-03	0.0	3.97479D-03	1.84002D-03
CM243	4.78435D-04	5.29514D-04	5.19111D-04	0.0	5.19111D-04	5.12432D-06
CM244	2.08181D-02	2.35532D-02	2.28431D-02	0.0	2.28431D-02	3.51743D-04
CM245	4.49434D-03	4.78135D-03	4.78135D-03	0.0	4.78135D-03	0.0
CM246	1.64706D-03	1.75213D-03	1.75213D-03	0.0	1.75213D-03	7.04731D-19
LFPP3	2.49599D-05	2.65193D-03	2.65193D-03	0.0	2.65193D-03	2.62541D-03
LFPP5	4.51645D-03	4.79562D-01	4.79562D-01	0.0	4.79562D-01	4.74767D-01
LFPP9	4.22871D-01	4.49550D+01	4.49550D+01	0.0	4.49550D+01	4.45055D+01
DUMP1	2.30537D-07	6.67450D-06	7.30061D-06	0.0	7.30061D-06	7.30061D-06
DUMP2	0.0	9.42982D-05	9.42982D-05	0.0	9.42982D-05	9.42982D-05

ISOTOPE	RECOVERED IN REPROCESSING	REPROCESSED AND USED IN MAKEUP	REPROCESSED AND SOLD	EXTERNAL FEED USED IN MAKEUP	AFTER FABRICATION	AFTER STORAGE (NEW CHARGE)
U-234	1.64705D-05	1.64705D-05	7.90057D-21	0.0	9.37410D-04	9.37410D-04
U-235	2.45151D-02	2.45151D-02	1.08331D-17	1.31929D+00	1.34330D+00	1.34335D+00
U-236	3.78017D-03	3.78017D-03	2.03987D-18	0.0	3.78017D-03	3.78017D-03
U-238	2.03481D+01	2.03481D+01	1.12351D-14	6.66746D+02	6.87094D+02	6.87094D+02
PU238	3.15395D-01	2.96733D-01	1.83619D-02	0.0	2.96710D-01	2.96710D-01
NP237	3.88512D-01	3.65467D-01	2.30453D-02	0.0	3.65467D-01	3.65467D-01
PU236	2.69052D-06	2.52939D-06	1.60632D-07	0.0	2.29536D-06	2.29536D-06
PU239	5.81301D+01	5.47017D+01	3.42843D+00	0.0	5.47017D+01	5.47017D+01
PU240	1.85196D+01	1.74132D+01	1.10644D+00	0.0	1.74135D+01	1.74135D+01
PU241	2.16910D+00	2.03953D+00	1.29575D-01	0.0	2.00142D+00	2.00142D+00
PU242	9.72712D-01	9.14439D-01	5.82729D-02	0.0	9.14439D-01	9.14439D-01
AM241	0.0	0.0	0.0	0.0	3.81072D-02	3.81072D-02
AM242	0.0	0.0	0.0	0.0	0.0	0.0
AM243	0.0	0.0	0.0	0.0	0.0	0.0
CM242	2.13477D-03	2.00696D-03	1.27805D-04	0.0	1.07790D-03	1.07790D-03
CM243	5.13957D-04	4.83200D-04	3.07860D-04	0.0	4.78435D-04	4.78435D-04
CM244	2.24914D-02	2.11435D-02	1.34776D-03	0.0	2.08181D-02	2.08181D-02
CM245	4.78135D-03	4.49493D-03	2.86526D-04	0.0	4.49493D-03	4.49493D-03
CM246	1.75213D-03	1.64713D-03	1.04993D-04	0.0	1.64713D-03	1.64713D-03
LFPP3	2.65193D-05	2.49599D-05	1.55933D-06	0.0	2.49599D-05	2.49599D-05
LFPP5	4.79562D-03	4.51647D-03	2.79157D-04	0.0	4.51647D-03	4.51647D-03
LFPP9	4.49550D-01	4.22871D-01	2.66795D-02	0.0	4.22871D-01	4.22871D-01
DUMP1	0.0	0.0	0.0	0.0	2.30541D-07	2.30541D-07
DUMP2	0.0	0.0	0.0	0.0	0.0	0.0

Note: The REBUS calculation was performed in 1/6th core geometry, multiply
the above numbers by 6 to get the total reactor massflow.

TABLE 6. Impact on Core Neutronics Performance of
Varying Pyroprocessing Removal Factors

Parameter	Reference Core	Modified Core
Fissile Loading[1] (kg/y)	348	344
Breeding Ratio[1]	1.074	1.081
Burnup Swing (%Δk)	0.73	0.69
Core Power Fraction		
BOEC	80.75	81.49
EOEC	75.35	76.00
Peaking Heat Rating (kw/ft)	12.1	12.2

[1] Fissile defined as U235+Pu239+Pu241 for purpose of this comparison.

TABLE 7. Impact on Core Neutronics of Actinide Total Recycle
with Partial Lanthanide Recycle

	Case No.							
	1	2	3	4	5	6	7	8
Am Recycled	No	Yes	Yes	Yes	Yes	Yes	Yes	Yes
F_e, %	0	0	1	5	20	20	33	75
(R, %)	(0)	(0)	(3.0)	(13.8)	(43.1)	(43.1)	(59.9)	(90.1)
Transmutation Feed	–	Core	Core	Core	Core	Blkt	Core	Core
Charged Mass, kg/y								
F.P.	0.0	0.0	2.55	13.3	63.5	67.4	127.2	808
H.M., x 10^3	4.59	4.59	4.59	4.57	4.52	4.52	4.46	3.78
Core Fissile	337	334	334	335	339	338	344	397
Cycle Reactivity Swing, %Δk	0.700	0.639	0.654	0.705	0.931	0.890	1.220	3.827
Reactor B.R.	1.076	1.082	1.081	1.076	1.056	1.058	1.031	0.777

TABLE 8. Impact on Core Neutronics Performance of Adding Blankets to Achieve High Breeding Ratio

Parameter	Fissile Self Sufficient Core	High Breeding Core
Axial Blk Thickness (in.)	0	14
Rows of Radial Blk	1	3
Residence Time		
Driver	4	4
Internal Blk	4	4
Radial Blk Row 1	4	6
2	–	9
3	–	12
Breeding Ratio		
Driver	0.436	0.425
Internal Blk	0.469	0.508
Radial Blk	0.228	0.482
Axial Blk	–	0.139
Total	1.133	1.553
Burnup Swing (%Δk)	0.16	0.45
Core Power Fraction (%)		
BOEC	78.9	73.2
EOEC	72.8	66.8
Pk Heat Rating (kw/ft)	12.4	11.1
Pk Discharge Blk MWd/kg	147.6	134.2
Pk Fast Fluence (10^{23} mvt)	3.43	3.13

TABLE 9. Effect of U236 Buildup on Neutronics Performance

	Charged Fuel Composition		
	Transition with U-236 (A)	Transition without U-236 (B)	Equilibrium (C)
Isotope Mass in Core Loading, kg			
U-235	108.70	106.3	3.1
U-236	70.7	0.0	0.0
U-238	1447.6	1525.2	1545.5
Pu-239	299.6	295.0	360.3
Pu-240	41.5	40.9	56.9
Pu-241	3.3	3.2	4.7
Pu-242	0.3	0.3	0.5
Burnup Reactivity Swing, %Δk	1.647	1.401	1.158
Breeding Ratio			
Driver	0.391	0.414	0.460
Internal Blanket	0.323	0.325	0.348
Radial Blanket	0.201	0.202	0.2167
Total	0.915	0.941	1.023
Net Fissile[a] Gain, kg/y	-21.9	-15.1	+6.2
BOC Power Fraction, %			
Core	82.95	82.70	81.83
Internal Blanket	11.12	11.31	11.90
Radial Blanket	4.60	4.65	4.88

[a]Fissile = $U^{25} + Pu^{49} + Pu^{41}$.

TABLE 10. Reactivity Coefficients for Equilibrium Pu-Fueled and
Startup U-Fueled Cores

	BOL U Startup	EOEC Pu Fueled	U Core/ Pu Core
Sodium Void Worth[a], (%Δk)			
Driver	-0.31	+1.31	-0.24
Int. Blanket	+0.36	+0.79	0.46
Rad. Blanket	-0.15	-0.054	2.78
Fuel Doppler Coefficient[a], $-10^{-3}T\frac{dk}{dT}$			
Flooded Doppler			
Driver	1.257	1.344	0.94
Int. Blanket	1.141	1.288	0.89
Rad. Blanket	0.360	0.347	1.04
Driver Axial Expansion Coefficient[b], (%Δk/cm)	-0.25	-0.26	0.96
Radial Expansion Coefficient[b], (%Δk/cm)	-0.52	-0.57	0.91
Control Rod Expansion Coefficient[c], (%Δk/cm)			
Primary Rods In[d]	+0.092	–	–
Primary Rods Out	+0.037	0.029	1.28
Beta-Effective	7.06-3	3.38-3	2.09
Prompt Lifetime, s	2.91-7	2.88-7	1.01

[a]Computed using first-order perturbation theory and 20 energy groups.
[b]Determined from 20-group eigenvalue calculations.
[c]Determined from 8-group eigenvalue calculations.
[d]Rods inserted to critical position.
[e]Assumed equal to BOEC value.